# Environmental Modelling
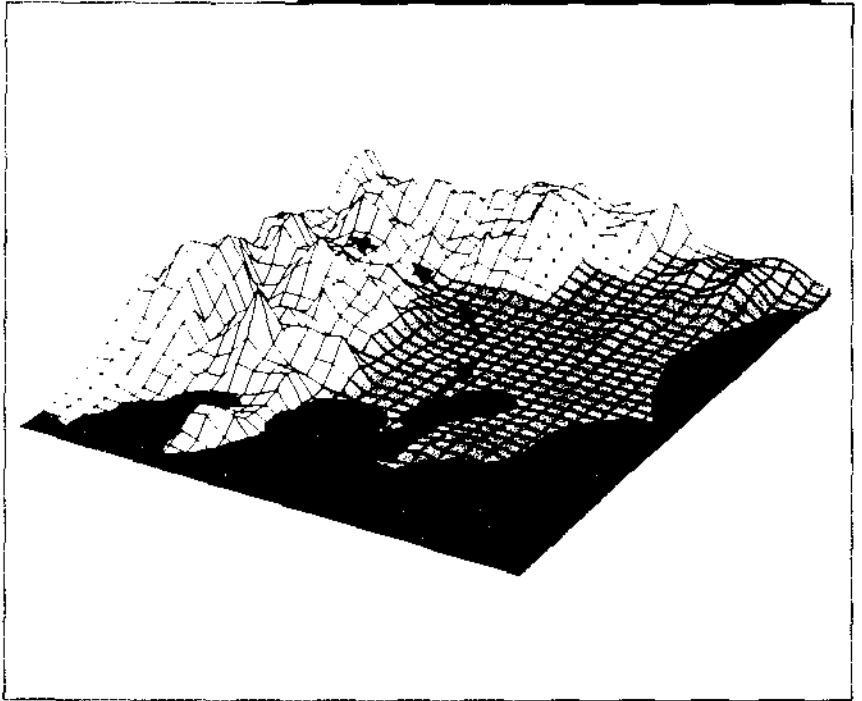
Editors: P. Melli
and P. Zannetti

Computational Mechanics Publications
Elsevier Applied Science

# CONTENTS

# Chapter 4

# Some Recent Advances in Computer Modeling of Groundwater Contaminant Transport

T.V. Hromadka II
*Williamson and Schmid, Irvine, CA 92714 and Department of
Mathematics, University of California, Fullerton, CA 92634, USA*

## Abstract

Recently advanced techniques in modeling groundwater contaminant transport include Boundary Element Methods and the more recent Complex Variable Boundary Element Method (CVBEM). In this chapter, the CVBEM is reviewed and then applied to a suite of practical case studies. Problems considered include contaminant transport between contaminant sources and pumping wells, landfill sites and pumping wells, and the influence of injection wells on contaminant transport. These recent numerical advances suggest future promise in the use of computer modeling techniques to develop solutions for mitigating contaminant transport.

## 4.1 Purpose of Chapter

The purpose of this chapter is to report on the advances made in using the Complex Variable Boundary Element Method (or CVBEM) in the approximation of conservative specie contaminant transport problems. Specifically, the CVBEM is a numerical boundary integral equation technique that is useful in describing flow characteristics of solute transport (for conservative specie transport that are transported by groundwater flow hydraulics (advection)) such as flow paths and steady groundwater flow timing properties. In this chapter, the use of the CVBEM in contaminant transport problems is extended by employment of a coupled least-squares optimization fit ($L^2$) and collocation fit in meeting the problem's prescribed boundary conditions. Because the CVBEM utilizes approximation functions that exactly solve the Laplace equation, there is no error in satisfying the governing potential flow linear operator equation except in meeting prescribed boundary conditions. The coupled $L^2$/Collocation error approach results in another technique to minimize this approximation error. The "approximate boundary" associated to the CVBEM solution (i.e., the locus of points

where the CVBEM solution achieves the prescribed boundary condition values) is used to graphically demonstrate the accuracy of the CVBEM model in achieving the solution to the groundwater flow problem.

## 4.2 Mathematical Model Development

Several publications develop the CVBEM in depth, and the reader is directed to Hromadka and Lai[1] for a thorough treatment of the numerical technique including FORTRAN computer codes to implement the technique. Publications that focus upon use of the CVBEM in contaminant transport problems include Hromadka and Yen[2] and Yen and Hromadka[4]. In all of these prior works, the CVBEM is based upon a collocation technique in meeting boundary condition values. Use of an $L^2$ norm with the CVBEM can be found in Hromadka and others[3]. The current chapter is the first report of a coupled $L^2$/Collocation method in matching boundary conditions by the CVBEM. A major advantage of the $L^2$/Collocation method over just $L^2$ or Collocation alone, is that the CVBEM "approximate boundary" (see Hromadka and Lai, 1987) is more readily developed (primarily at the interface between prescribed groundwater flow potential and normal flux boundary conditions), and the departures (i.e., distance) between the approximate and true problem boundaries are diminished over use of the Collocation method alone.

## 4.3 Complex Variable Boundary Elements (CVBEM)

The CVBEM is a numerical approximation of the Cauchy integral formula of an analytic function $\omega(z)$ over a domain $\Omega$ and simple closed contour $\Gamma$ within $\Omega$,

$$\omega(z) = \frac{1}{2\pi i} \int_\Gamma \frac{\omega(\zeta) d\zeta}{\zeta - z} \tag{1}$$

where $\omega(z) = \phi(z) + i\psi(z)$; $\phi(z)$ is the two-dimensional potential function and $\psi(z)$ is the two-dimensional conjugate of $\phi(z)$; and where at least one point value of $\phi(z)$ and $\psi(z)$ are known on $\Gamma$.

Flux values of the potential, $\phi(z)$, on $\Gamma$ are related to $\psi(z)$ by the Cauchy-Riemann relationship

$$\left|\frac{\partial \phi}{\partial n}\right| = \left|\frac{\partial \psi}{\partial s}\right| \tag{2}$$

where n and s are normal and tangential vector components along $\Gamma$, respectively.

Equation (1) is approximately solved by use of (for example) one-dimensional spline functions of $\phi(z)$ and $\psi(z)$ defined on small segments (boundary elements, $\Gamma_j$) of $\Gamma$. Nodal points, with coordinates $z_j, j = 1, 2, \cdots, n$, are placed on $\Gamma$, and each boundary element $\Gamma_j$ is a straight-line segment with endpoints $z_j$ and $z_{j+1}$. A global approximation function of $\omega(z)$ on the union of boundary elements, $U\Gamma_j$ is defined by $G_1(z)$ where

$$G_1(z) = \sum_{j=1}^{n} N_j(z) \omega j \tag{3}$$

where $\omega_j = \phi_j + i\psi_j$ are nodal point $j$ values of $\omega(z_j), \phi(z_j), \psi(z_j)$; and $N_j(z)$ is a piecewise linear complex polynomial satisfying for all $z \in U\Gamma_j$:

$$N_j(z) = \begin{cases} 1, & z = z_j \\ 0, & z = z_{j-1}, z_{j+1} \\ 0, & z \notin \Gamma_{j-1} \cup \Gamma_j \end{cases} \tag{4}$$

Substituting the $G_1(z)$ approximation (the subscript 1 refers to a first-order spline function family) into the Cauchy integral equation results in

$$\hat{\omega}_1(z) = \frac{1}{2\pi i} \int_\Gamma \frac{G_1(\zeta)d\zeta}{\zeta - z} \tag{5}$$

where $\hat{\omega}_1(z)$ is the CVBEM approximation, which is a linear combination of n pairs of nodal point values $\phi_j$ and $\psi_j$, wherein n values are known via prescribed boundary conditions, leaving no more than n unknown nodal point values. Convergence of $\hat{\omega}_1(z)$ to the exact solution of the potential flow problem (i.e., steady state groundwater or advective contaminant transport) depends on the uniform convergence of $G_1(z)$ to $\omega(z)$ on $\Gamma$.

The aforementioned references present two techniques in developing estimates for the unknown CVBEM nodal values by use of a collocation technique, and by use of a $L^2$ technique. The coupled $L^2$/Collocation technique is described in the following section of this chapter.

## 4.4 $L^2$/Collocation

The CVBEM approximation function, $\hat{\omega}_1(z)$, based upon first order spline functions, can be written as (for problems unsolved by a first order complex polynomial)

$$\hat{\omega}_1(z) = \sum_{j=1}^n C_j(z - z_j)\mathrm{Ln}(z - z_j) \tag{6}$$

where Ln is the complex natural logarithm function and $C_j$ are complex constants $C_j = \alpha_j + i\beta_j$ for $j = 1, 2, \cdots, n$. A collocation technique to solving for the CVBEM unknown constants (i.e., unknown nodal values) is to set implicit relationships (Hromadka and Lai, 1987)

$$\begin{align} \mathrm{Im}(\hat{\omega}(z_j)) &= \hat{\psi}(z_j) \\ &\tag{7} \\ \mathrm{Re}(\hat{\omega}(z_j)) &= \hat{\phi}(z_j) \end{align}$$

where Im and Re are the imaginary and real components of $\hat{\omega}(z_j)$, respectively, and $\hat{\psi}(z_j)$ or $\hat{\phi}(z_j)$ are the unknown nodal values, respectively. Such an implicit relationship results in a Fredholm equation of the second kind.

An $L^2$ relationship is to minimize the integral objective function, $\mathcal{X}$,

$$\mathcal{X} = \int_{\Gamma_\phi} (\hat{\phi} - \phi)^2 \ d\Gamma + \int_{\Gamma_\psi} \left( \frac{\partial \hat{\psi}}{\partial s} - \frac{\partial \psi}{\partial s} \right)^2 \ d\Gamma \tag{8}$$

where $\Gamma_\phi$ and $\Gamma_\psi$ refer to the prescribed potential and normal flux boundary conditions, respectively. The numerical procedure for minimizing $\mathcal{X}$ can be found by the usual Gram-Schmidt procedures as discussed in Hromadka and others (1987).

The coupled $L^2$/Collocation procedure is a four step process:

1. Locate all "interface" nodal points on $\Gamma$ wherein both $\phi$ and the normal derivative of $\phi$ are known.

2. At all interface nodal points, $z_k$ , set dual nodal equations:
   $\text{Re}\ (\hat{\omega}(z_k)) = \phi(z_k) = \phi_k$
   $\text{Im}\ (\hat{\omega}(z_k)) = \psi(z_k) = \psi_k$
   where both $\phi_k$ and $\psi_k$ are known nodal values.

3. At all non-interface nodal points, solve for unknown nodal values by the $L^2$ formulation (excluding the interface nodal points already solved).

It is noted that the resulting CVBEM approximation function is equivalent to just the $L^2$ approach with massive weighting of CVBEM nodal values at the aforementioned "interface" type nodal points on $\Gamma$. Additionally, this CVBEM approximation exactly achieves the problem boundary conditions at these "interface" nodal points on $\Gamma$.

An additional fourth step is used for computational purposes in developing the CVBEM "approximate boundary" (see next section):

4. At all boundary corners (or locations in $\cup \Gamma_j$ where $\Gamma_{j-1}$ and $\Gamma_j$ join at an angle $\theta \neq \pi$ at $z_j$), collocate the known boundary condition (say $\phi_j$ is known at $z_j$) to equate to $\hat{\omega}(z_j)$:
   $\text{Re}(\hat{\omega}(z_j)) = \phi_j$
   or similarly,
   $\text{Im}(\hat{\omega}(z_j)) = \psi_j$
   where $\phi_j$ (or $\psi_j$) is known at $z_j$.

## 4.5 Approximate Boundary

The CVBEM approximation function $\hat{\omega}(z) = \hat{\phi}(z) + i\hat{\psi}(z)$ has the property that both $\hat{\phi}(z)$ and $\hat{\psi}(z)$ exactly solve the Laplace equation in the interior of $\Omega$, both are continuous functions on $\Gamma$, and both are conjugate functions. Additionally, depending on the success in the numerical model by placement and number of nodal points on $\Gamma$ (and hence the goodness of fit of $G_1(z)$ to $\omega(z)$ on $\Gamma$), $\hat{\phi}(z) \simeq \phi(z)$ on $\Gamma_\phi$ and $\hat{\psi}(z) \simeq \psi(z)$ on $\Gamma_\psi$. The "approximate boundary" concept graphically demonstrates the success in $\hat{\omega}(z)$ matching the prescribed boundary condition values by the development of the

approximate boundary, $\hat{\Gamma}$, which is the locus of points where $\hat{\omega}(z)$ achieves the boundary condition values. (Hromadka and Lai (1987) develop the approximate boundary concept in detail.)

From steps (2) and (4) of the previous section, one is guaranteed that $\hat{\Gamma}$ and $\Gamma$ coincide at all "interface" nodal points and all corners of $U\,\Gamma_j$ (and hence corners of $\Gamma$). Excluding corners of $U\,\Gamma_j$, let $z^*$ be a point on $\Gamma$ (which is a straight-line segment in a neighborhood of $z^*$). Then the approximate boundary is located with normal and tangential coordinates $(n,s) = (n^*,s^*)$ such that $z^* = (0,s^*)$ and $|\,n^*\,|$ is the normal distance betweeen $\hat{\Gamma}$ and $\Gamma$ with $s = s^*$. $\hat{\Gamma}$ is found by locating where $\hat{\phi}(n^*,s^*) = \phi(0,s^*)$ on $\Gamma_\phi$ and where $\hat{\psi}(n^*,s^*) = \psi(0,s^*)$ on $\Gamma_\psi$ (or where $\frac{\partial \hat{\psi}}{\partial s}(n^*,s^*) = \frac{\partial \psi}{\partial s}(0,s^*)$ on $\Gamma_\psi$). It is apparent that at all "interface" nodes, $\hat{\omega}(0,s^*) = \omega(0,s^*)$, and hence $\hat{\Gamma}$ and $\Gamma$ intersect at interface nodes, by step (2) of the $L^2$/Collocation procedure.

Using a dense set of $(0,s^*)$ point locations on $\Gamma$, the approximate boundary $\hat{\Gamma}$ is found, that corresponds to the CVBEM $\hat{\omega}(z)$, and the goodness of the CVBEM approximation is readily seen by comparing $\hat{\Gamma}$ and $\Gamma$. Should $\hat{\Gamma} = \Gamma$ everywhere, then $\hat{\omega}(z) = \omega(z)$ on $\Omega \cup \Gamma$. Additionally, if the analyst is willing to accept $\hat{\Gamma}$ as the "true" boundary of the problem, then $\hat{\omega}(z)$ is the "true" solution of the redefined boundary value problem.

## 4.6 Sources and Sinks

The CVBEM develops an analytic function on $\Omega$. Sources and sinks are introduced by adding the complex logarithm function $\ln(z - z_r)$ (Yen and Hromadka, 1986) for each source sink at location $z_r$, to the CVBEM approximation function, $\omega(z)$. The composite CVBEM approximation is analytic everywhere in $\Omega$ except for all locations $z_r$, and the branch-cut originating from each $z_r$.

## 4.7 Application to Advective Contaminant Transport Problems

In order to demonstrate the above described procedures, three selected contaminant transport problems are considered.

### Source-Sink Problem

In this illustrative problem, a simple groundwater well and injection well are installed in a flow-field. Figures 4.1a,b,c demonstrate the approximate boundary $\hat{\Gamma}$ developed from use of CVBEM approximations for three different nodal point configurations. In Figure 4.1c, the closeness of $\hat{\Gamma}$ to $\Gamma$ suggests that the underlying CVBEM approximation function is a good estimator of the background potential problem. And if $\hat{\Gamma}$ is acceptable as the "true" problem boundary, then the CVBEM approximation would be the exact solution. The Figure 4.1c model is developed by adding 16 nodal points to the CVBEM model of Figure 4.1b, focusing at the domain corners near the source and sink.

## Landfill Evaluation: Injection-Well Problem

Figure 4.2 depicts the application of the CVBEM and approximate boundary techniques to a landfill contaminant transport problem. A set of injection wells are used to divert contamination of potable water from a nearby landfill site. Injection wells are considered to offset the effects of contaminant flow to the potable water. Figures 4.2a,b,c provide the problem definition, and two CVBEM models of the problem and resulting approximate boundaries. The Figure 4.2b CVBEM model approximate boundary was used to locate additional CVBEM nodes in an effort to reduce approximation error. In Figure 4.2c, the addition of CVBEM nodal points improves the modeling accuracy as manifested by the reduction in departure between the approximate boundary, $\hat{\Gamma}$, and the true boundary, $\Gamma$. The maximum departure of 40 m between $\hat{\Gamma}$ and $\Gamma$ in Figure 4.2c, is negligible in comparison to the overall scale of the problem; that is, the magnitude of difference between energy head values along $\Gamma$ are minor. The CVBEM model of Figure 4.2c is seen to be a good approximation of the true problem conditions. Use of this 70-node CVBEM model could be used to develop streamlines and flow velocity calculations, among other factors. In the following two applications, the CVBEM landfill contaminant transport problem is further studied regarding contaminant arrival times.

## Contaminant Transport Arrival Time

Figure 4.3 demonstrates the use of the CVBEM to estimate transport time along streamlines. Case A evaluates arrival time of the contaminant to a pumping well, whereas Case B evaluates the effect of injection wells in slowing the arrival time. As in all the above applications, the CVBEM is used based upon the Generalized Fourier Series Approach of Equation (8).

**Application A.** Here we will consider the steady flow produced by a single pumping well (50 m$^3$/hr) near a landfill site with an equipotential boundary ($\phi = 2$ m) along the coordinate y=1000 m. As shown in Figure 4.3, it takes the contaminant front produced by the landfill 9.0 years to reach the pumping well.

**Application B.** When two injection wells are installed between the landfill and the pumping well, their influence on retarding the contaminant movement can be assessed. When 10 m$^3$/hr is injected at each well it takes more than 13 years for the contaminant front to reach the pumping well (see Figure 4.4).

The results of Figures 4.3 and 4.4 are based upon a 75-node CVBEM model. Additionally, the approximate boundaries $\hat{\Gamma}$ for each CVBEM model deviated only a few meters from the true problem boundary shape, $\Gamma$, and from the geometry of the landfill boundary. That is, $\hat{\Gamma}$ deviated from $\Gamma$ well within the measuring tolerance possible in the field. Hence, the CVBEM results are exact should $\hat{\Gamma}$ be considered the true geometry of the problem. The $L^2$/Collocation approach was useful in these applications due to the reduction in effort needed to develop the approximate boundaries for numerical error evaluation and subsequent CVBEM model fine-tuning.

## 4.7 Conclusions

The CVBEM is applied to groundwater advection contaminant transport problems, and the CVBEM numerical error is evaluated by use of the approximate boundary graphical technique. Besides providing actual solutions to many groundwater flow and advective contaminant transport problems, the CVBEM can be used to develop analytic test cases to be used in numerically calibrating other groundwater and contaminant transport numerical models for other classes of problems. In this chapter, the CVBEM model is developed by the use of a coupled $L^2$/Collocation fit to prescribed boundary conditions.

The coupled $L^2$/Collocation method used in the CVBEM results presented herein was found to be useful in the development of the approximate boundary. The $L^2$/Collocation method was similar in computational effort to either the $L^2$ or Collocation approaches separately, but significantly simplified the plotting and definition of approximate boundaries corresponding to the CVBEM models.

## References

1. Hromadka II, T.V. and Lai, Chintu, The Complex Variable Boundary Element Method In Engineering Analysis, Springer-Verlag Publishers, 1987.

2. Hromadka II, T.V. and Yen, C.C., 1986, A Model of Groundwater Contaminant Transport Using the CVBEM, Int. Journal of Computational Mechanics, Vol. 1, pp. 105-113, Springer-Verlag Publishers.

3. Hromadka II, T.V., Yen, C.C., and Pinder, G.F., 1987, The Best Approximation Method - An Introduction, Springer-Verlag Publishers. Lecture Notes Series, Number 27.

4. Yen C.C. and Hromadka II, T.V., 1986, Complex Variable Boundary Element Solution of Groundwater Contaminant Transport, Proceedings: Envirosoft '86 Conference, Computational Mechanics Press, pp. 409-420.
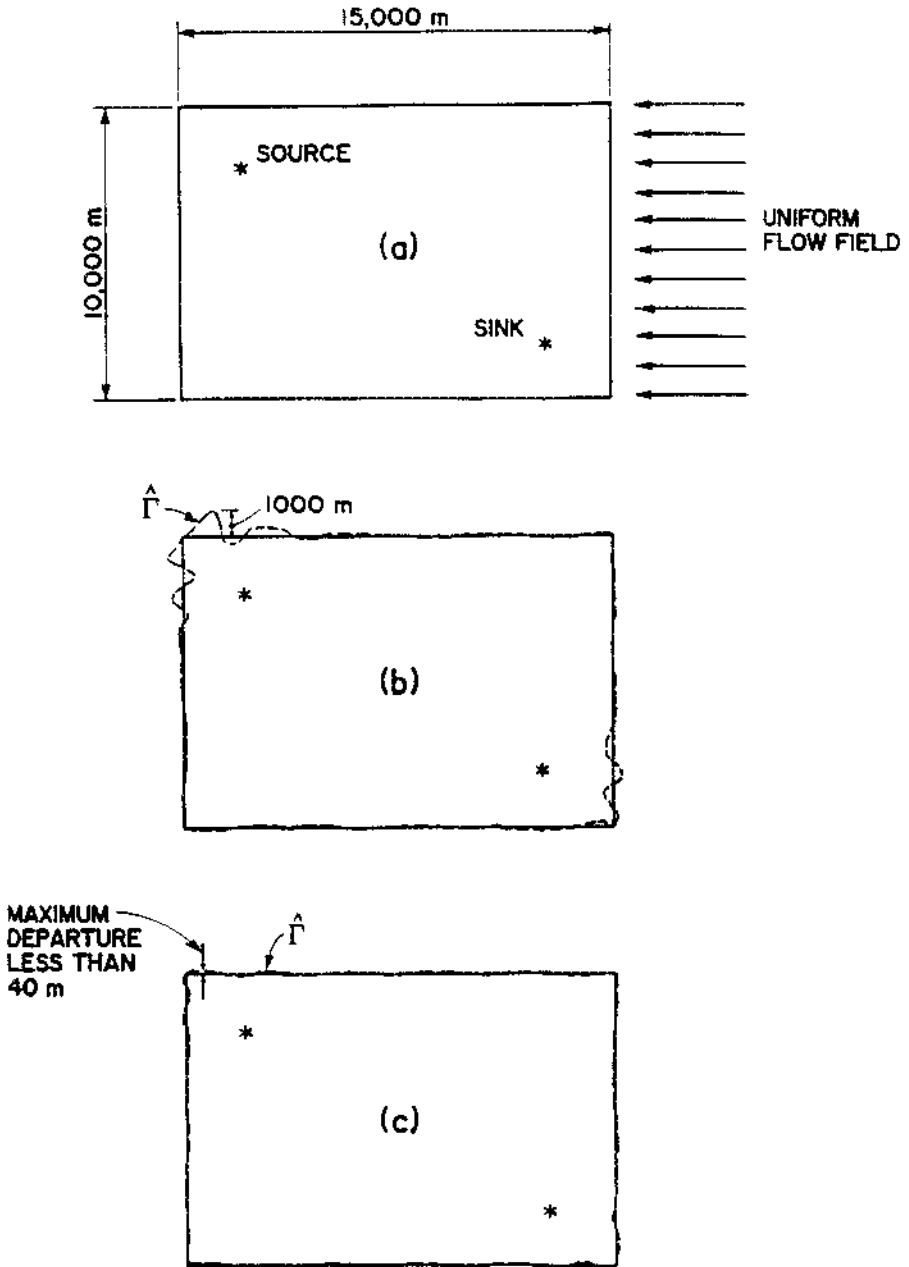
Figure 4.1a: Problem Definition,
      b: CVBEM approximate boundary for 50 nodes on $\Gamma$,
      c: CVBEM approximate boundary for 66 nodes on $\Gamma$.
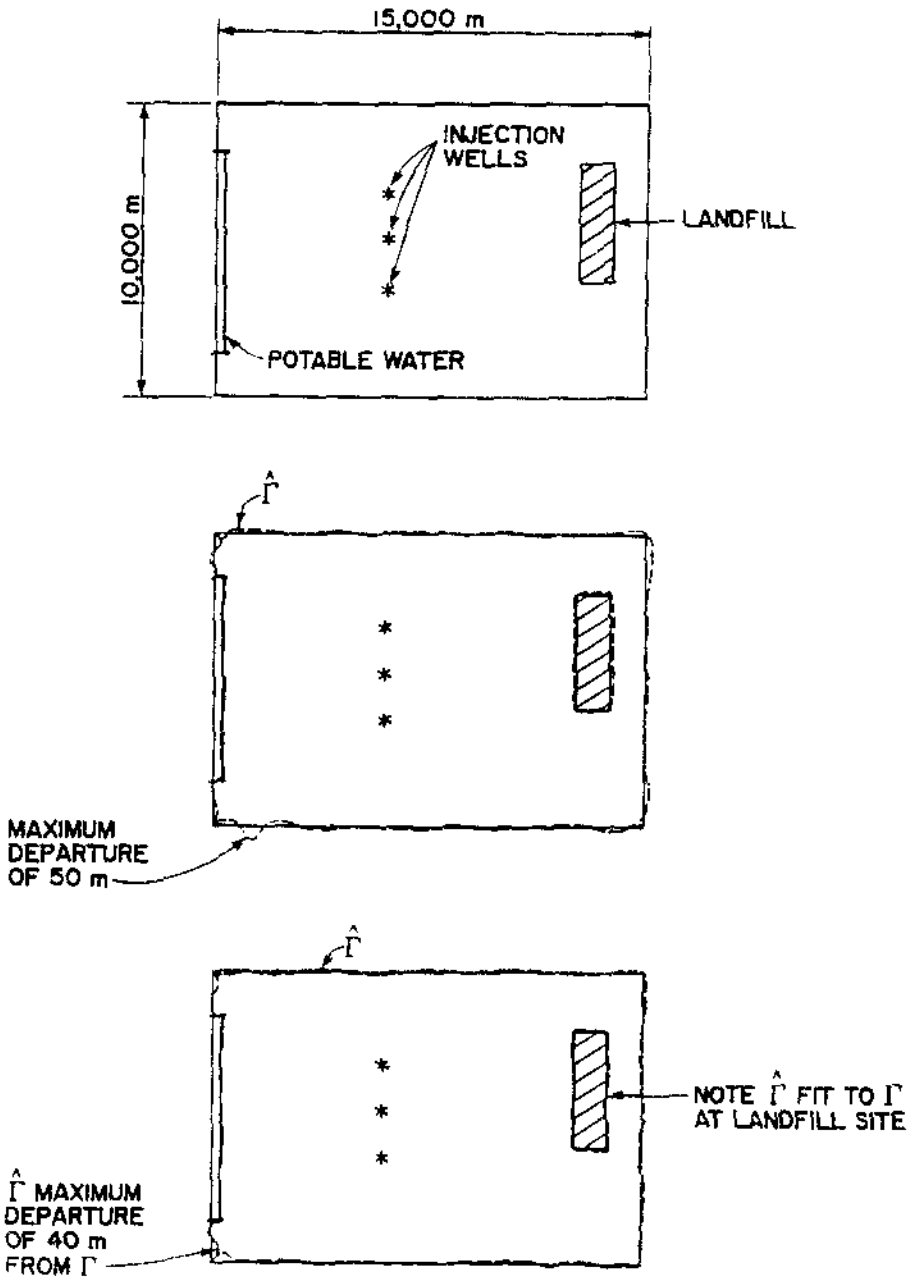
Figure 4.2a: Problem Definition.
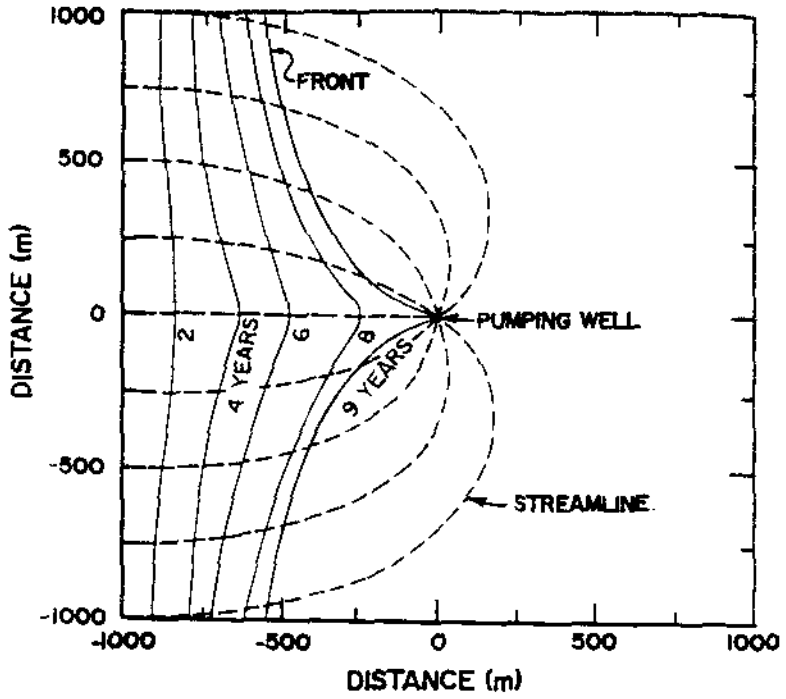       b: CVBEM approximate boundary for 60 nodes,
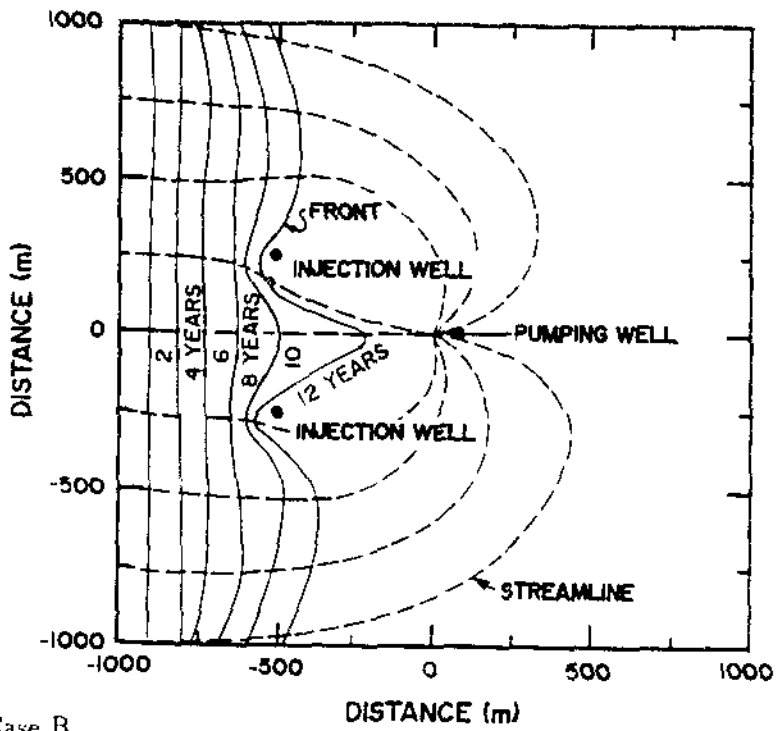       c: CVBEM approximate boundary for 70 nodes.

Figure 4.3: Case A



Figure 4.4: Case B